

## Hot Steady-State FRCs and the Field Reversed Mirror Concept

A.L. Hoffman, H.Y. Guo, R.D. Milroy, R. Farengo\*, H. Ferrai\*

Redmond Plasma Physics Laboratory, University of Washington, Seattle, WA, USA

\*Centro Atomico Bariloche (CNEA) & Instituto Balseiro, S.C. de Bariloche, RN, Argentina

e-mail contact of main author: [hoffman@aa.washington.edu](mailto:hoffman@aa.washington.edu)

**Abstract:** The reactor advantages of a linear, naturally high beta configuration would be enormous, which is the reason for original interest in the field-reversed-mirror (FRM) concept. Attempts to reverse the axial magnetic field of simple mirror plasmas using tangential neutral beam injection (TNBI) were unsuccessful, but creating energetic ion rings within an already formed field-reversed-configuration (FRC) is completely straightforward. Appropriate hot, steady-state FRCs can now be formed using rotating magnetic fields (RMF) and scaling laws are developed for achievable RMF sustained FRC flux levels. Calculations are presented for TNBI showing the flux levels necessary for energetic ion trapping, how to achieve them using RMF, and the efficiency of energetic ion ring generation in such RMF produced FRCs.

### 1. Introduction

The field reversed mirror (FRM) was one of two ideas originally pursued for reducing the end-losses from standard mirror plasmas.[1] Due to the inability to reverse the axial magnetic field using tangential neutral beam injection (TNBI),[2] only the second idea, the tandem mirror, was seriously developed. Recent advances in creating stable, hot, steady-state field reversed configuration (FRC) plasmas (sketched in Fig. 1) using rotating magnetic fields (RMF) make this an appropriate time for re-examining the FRM concept. A low density, hot FRC makes an ideal trap for TNBI produced charge-exchange ions, and the process of adding energetic ion rings to the FRC is completely straightforward. However, more FRC flux is required for efficient ion trapping within the FRC than is available in present small-scale experiments. The RMF process for creating the original FRC, and for building up and sustaining the poloidal flux is now well understood, and simple scaling laws show how to reach the flux levels necessary for TNBI ion ring production to be effective. The combination of RMF and TNBI would be ideal for flux build-up and sustainment, plasma heating, and most importantly, providing stability to FRC/FRM plasmas. The scaling laws for required flux values and TNBI ring generation efficiency, as well as the means for reaching these flux levels, are given in this paper.

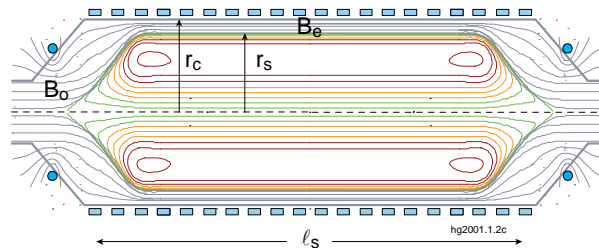


Figure 1. FRC geometry inside flux conserver.

### 2. RMF Current Drive Scaling

RMF current drive was developed in a long series of rotamak (spherical FRC) experiments by Ieuan Jones' group at Flinders University,[3] and later extended to more standard prolate FRCs inside flux conservers in the TCS (Translation, Confinement, Sustainment) experiments at the University of Washington.[4] The recently upgraded TCS (TCSU) produces  $r_s \sim 37$  cm radius,  $\ell_s \sim 1.5$  m long FRCs inside a  $r_c = 42$  cm radius flux conserver with external (to the FRC)  $B_e = 30$  mT magnetic fields. The plasma density is  $n_e \sim$

$10^{19} \text{ m}^{-3}$  and the total electron plus ion temperatures  $T_t = T_e + T_i \sim 200 \text{ eV}$ . The poloidal flux is  $\phi \sim 3.5 \text{ mT}$ .<sup>[5]</sup>

RMF works by building up flux as its torque on the electrons,  $\mathbf{T}'_{\text{rmf}}$  per unit antenna length, exceeds the resistive torque,  $\mathbf{T}'_{\eta}$  per unit FRC length, due to friction (resistivity) with ions, according to the relationship

$$\frac{d\phi_p}{dt} = 2\pi R E_{\theta}(R) = \frac{4}{\langle n_e \rangle e r_s^2} (\mathbf{T}'_{\text{rmf}} - \mathbf{T}'_{\eta}) . \quad [1]$$

$E_{\theta}(R)$  is the azimuthal electric field at the FRC field null  $R = r_s/\sqrt{2}$ .

$$\mathbf{T}'_{\text{rmf}} = \frac{2\pi r_s^2 B_{\omega}^2}{\mu_o} f(\zeta) , \quad [2]$$

and 
$$\mathbf{T}'_{\eta} = 1.16\pi r_s^2 e n_m \left( \frac{B_e}{\mu_o} \right) \langle \eta_{\perp} \rangle . \quad [3]$$

where  $B_{\omega}$  is the RMF magnitude,  $\eta_{\perp}$  is the cross-field plasma resistivity (highly anomalous) and  $f(\zeta)$  depends on the ratio  $\zeta$  of actual electron line current to the maximum possible RMF sustained line current,

$$\zeta = \frac{I'_{\text{line}}}{I'_{\text{sync}}} = \frac{2B_e/\mu_o}{0.5\langle n_e \rangle \omega r_s^2} = \frac{\langle \omega_e \rangle}{\omega} . \quad [4]$$

For RMF to drive the electrons the RMF frequency  $\omega$  must exceed the electron rotation frequency  $\omega_e$ . Calculations show  $f(\zeta)$  to be about equal to 0.1 for  $0.2 < \zeta < 0.95$ , and necessarily going to zero as  $\zeta$  approaches unity.<sup>[5]</sup>

For  $\zeta$  in the above range,  $\omega_e \sim \omega$  near the FRC separatrix (which allows the RMF to penetrate into the FRC), while a region with  $\omega_e < \omega$ , whose depth and breadth depends on  $\zeta$ , exists near the field null. Equating the RMF and resistive torques, and using  $B_e = (2\mu_o n_m k T_t)^{1/2}$ , ( $T_t$  is assumed uniform due to the present low flux levels), in steady-state the peak plasma density is

$$n_m (10^{20} \text{ m}^{-3}) = 1.4 \frac{B_{\omega}^{4/3} (\text{mT})}{T_t^{1/3} (\text{eV}) \langle \eta_{\perp} (\mu\Omega - \text{m}) \rangle^{2/3}} . \quad [5]$$

The above listed TCSU conditions, obtained with a  $B_{\omega} = 5 \text{ mT}$ , imply  $\langle \eta_{\perp} \rangle \sim 100 \mu\Omega\text{-m}$ . The FRC density is mostly determined by the RMF magnitude and the average cross-field resistivity, and is only weakly dependent on the plasma temperature, but in earlier TCS radiation dominated experiments with temperatures 5 to 10 times lower, typical densities were almost twice as high, in agreement with the Eq. (5) scaling. Plasma temperature is determined independently by overall power balance.

Using the above expressions, a useful relationship is

$$\frac{B_e}{B_{\omega}} = 7.4 \frac{(T_t (\text{eV})/n_m (10^{20} \text{ m}^{-3}))^{1/4}}{\langle \eta_{\perp} (\mu\Omega - \text{m}) \rangle^{1/2}} \quad [6]$$

A numerical result for the power absorbed per unit length due to the azimuthal currents is

$$P'_0(\text{W/m}) = 10.8 \langle \eta_{\perp} (\mu\Omega\text{-m}) \rangle B_c^2 (\text{mT}). \quad [7]$$

The absorbed power due to resistive dissipation is independent of plasma radius for a given magnetic field since a larger area is compensated by a lower current density. Experiments have shown that the resistivity is much higher near the outer edge of the FRC, presumably due to the higher electron drift velocity there,[6] and if inner and edge resistivities are specified as  $\eta_i$  and  $\eta_e$ , the average resistivities (based on simple current profile models) to be used in the torque based and power based expressions are  $\langle \eta_{\perp} \rangle_t = (0.73\eta_i + 0.27\eta_e)$  and  $\langle \eta_{\perp} \rangle_p = (0.58\eta_i + 0.42\eta_e)$ .  $\eta_e$  has a greater effect on the power absorption, which is proportional to the square of the current density. A value of  $\eta_e = 10\eta_i$  best fits all aspects of experimental data, and the value of  $D_{\perp i} = \eta_i/\mu_0$  should be characteristic of internal transport.

In reference to Eq. (6), the ratio  $B_e/B_{\omega}$  is plotted in **Fig. 2** as a function of  $(T_t/n_m)^{1/4}$ . Results are shown for both TCSU and TCS, and for some TCSU experiments run in Argon to illustrate that the difference between TCS and TCSU was indeed due to the lowering of impurity and radiation levels. Lines are drawn representing different values of the inner resistivity in accordance with Eq. (6). The absorbed power which is needed to sustain the FRC flux is obviously an important

quantity. Measurements at different ratios of  $B_e/B_{\omega}$  yield the relationship  $P'_{\text{abs}}(\text{W/m}) = 40 \times 10^3 B_{\omega}^2 (\text{mT}) + 1.2 \times 10^3 B_c^2 (\text{mT})$ . Comparing the latter term, related to the azimuthal currents, with Eq. (7) yields a value of  $\langle \eta_{\perp} \rangle_p = 110 \mu\Omega\text{-m}$ , or  $\eta_i = 23 \mu\Omega\text{-m}$ , about the same result as calculated from the torque analysis. The wave related power absorption, proportional to  $B_{\omega}^2$ , is useful for initial plasma heating, but will become less important as the ratio  $B_e/B_{\omega}$  increases (as it must to approach reactor parameters).

Although high energy ion contributions from either TNBI or fusion reaction products can contribute significantly to FRC current drive, the value of  $D_{\eta} = (\eta_{\perp}/\mu_0)$  is still key. Particle and energy transport will also be related to this flux diffusion parameter. Many theta pinch and FRC experiments have been modeled using a  $D_{\eta}$  value which is strongly dependent on the ratio of electron drift velocity,  $v_{de}$  to the ion thermal speed  $v_{ti}$ . A lower-hybrid-drift (LHD) formula with an algebraic dependence on  $\gamma_d \equiv v_{de}/v_{ti}$  has been very descriptive of

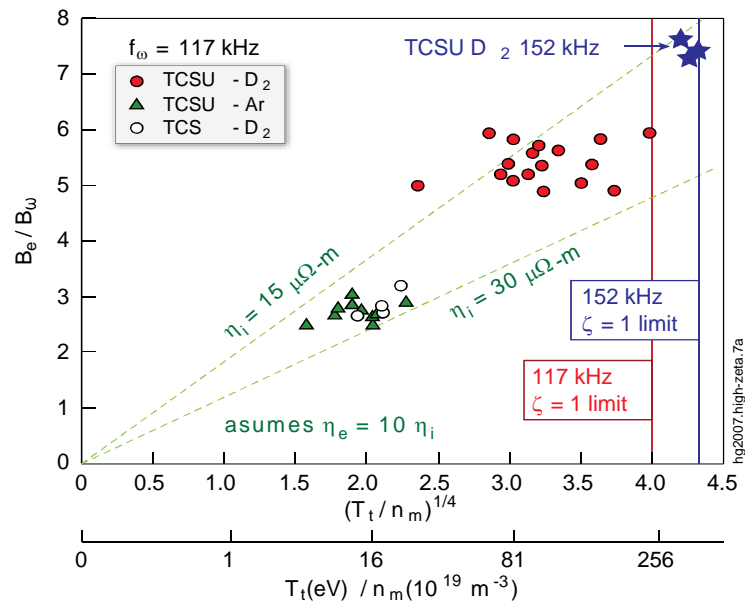


Figure 2. Measured ratios of poloidal field to applied RMF.

theta-pinch results,[7] while an exponential dependence (Chodura) has been used to describe both FRC formation and decay.[8] An expression for LHD turbulence was calculated several decades ago to explain theta-pinch diffusion.[9]

$$D_{LHD} = 0.15D_B \frac{\gamma_d^2}{1 + \frac{\pi}{8}\gamma_d^2} \quad [8]$$

$D_B(\text{m}^2/\text{s}) = T_e(\text{eV})/16B(\text{T})$  is the Bohm diffusion coefficient. Although Eq. (8) strictly applies to electrostatic drift waves in low  $\beta$  plasmas, we will use it for both the FRC low  $\beta$  edge region (where the observed  $\eta_{\perp}$  is highest) and for the electromagnetic type turbulence expected near the field null. It is the scaling with drift parameter that is key.

The values of  $D_{\eta} = \langle \eta_{\perp}/\mu_0 \rangle$  for TCS and TCSU Argon and Deuterium experiments, based on Eq. (6), are plotted in **Fig. 3** versus  $D_B$ . For the TCS and TCSU Argon experiments the plasmas were very collisional, with  $l_s/\lambda_{ii} < 1$ , and  $D_{\eta}$  follows Bohm scaling. However, the TCSU Deuterium plasmas were collisionless,  $l_s/\lambda_{ii} > 1$ , and  $D_{\eta}$  follows the  $D_{LHD}$ -like scaling of Eq. (8). The electron rotation velocity for a rigid rotor profile is  $\omega_{RR}(\text{rad/s}) = 4K_{RR}T_i(\text{eV})/B_e(\text{T})R^2(\text{m})$ . Using

$K_{RR} = 1.5$  typical of RMF sustained FRCs,  $v_{ti} = (kT_i/m_i)^{1/2}$  (actually closer to the ion sound speed), and the pressure balance relationship  $B_e = (2\mu_0 kT_i n_m)^{1/2}$ , the RR drift velocity ratio is

$$\gamma_d \equiv \frac{v_{de}}{v_{ti}} = \frac{0.2A_i^{1/2}}{n_m^{1/2}(10^{20} \text{ m}^{-3})r_s(\text{m})} \left( \frac{r}{r_s} \right). \quad [9]$$

For typical TCSU conditions with  $A_i = 2$ ,  $n_m = 1 \times 10^{19} \text{ m}^{-3}$ , and  $r_s = 0.37 \text{ m}$ ,  $v_{de}/v_{ti} = 2.3(r/r_s)$ . A value of 2.3 was used for the  $D_{LHD}$  line in Fig. 3. The drift velocity is actually even higher at the edge than for a simple RR distribution since the edge electrons rotate near synchronously with the RMF, while the central  $\omega_e < \omega_{RR}$ . This may be the reason why the FRC edge resistivity is seen to be so much higher than the interior resistivity.

The scaling of  $D_{\eta}$  with the drift parameter ratio is key to any FRC/FRM reactor scheme. The  $D_{LHD}$  type scaling of Eq. (8) is highly favorable, even better than gyro-Bohm, which only scales linearly with  $v_{de}/v_{ti}$ . Temperature is not a factor in the  $v_{de}/v_{ti}$  ratio, which scales as  $1/Rn^{1/2}$ . An experiment to test this scaling should increase  $Rn^{1/2}$  by at least a factor of 3, either by making  $r_s$  larger or  $n$  higher (by increasing  $B_0$ ). The results are likely to be exponentially favorable if  $\eta_{\perp}$  is reduced as expected.

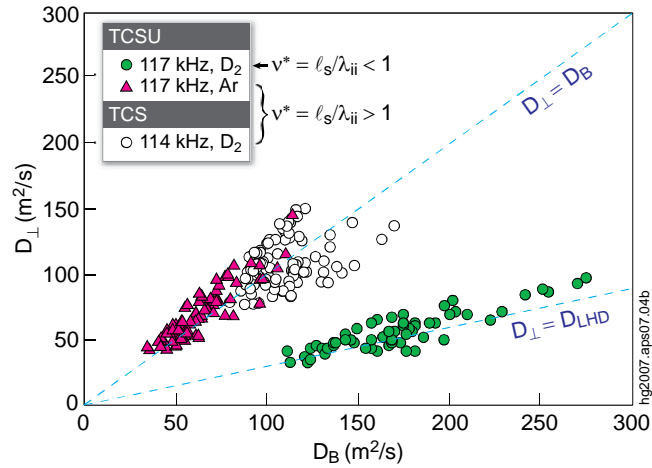


Figure 3. Average effective resistivities in RMF sustained FRCs.

Several recent numerical calculations of turbulent diffusion in diamagnetic plasmas exhibit the rapid transition from near classical to highly turbulent diffusion as the drift parameter ratio exceeds unity. Loverich and Shumlak observed the development of ion shocks in a sophisticated two-fluid code,[10] and similar effects were seen in gyrokinetic calculations by Rogers.[11] Near classical radial confinement was also recently reported in the Gamma-10 tandem mirror facility.[12] If all this experimental and theoretical work is borne out, the great promise of the FRC/FRM approach to fusion would be given a significant boost.

### 3. Tangential Neutral Beam Injection

Monte-Carlo calculations have been made for tangential neutral beam injection (TNBI) of deuterium atoms into an FRC for the purpose of determining ratios of generated energetic ion ring current to injected beam current,  $\alpha_{rb} = I_r/I_b$ . An FRC flux level was chosen which is about minimal for efficiently forming energetic ion rings with a deuterium beam energy of 10 keV. The numerical results can best be considered in terms of the characteristic ion energy  $E_{ic}$  which, when starting with a tangential velocity  $v_\theta = -v_{ic}$  at the field null ( $E_{ic} = 0.5m_i v_{ic}^2$ ), results in an orbit (A) which circles the FRC axis with minimum and maximum excursions equal to  $R$  and  $r_s$  as sketched in Fig. 4. This characteristic energy is [13]

$$E_{ic} \text{ (keV)} = \frac{0.0144}{A_i} \left( \frac{\phi_p \text{ (mWb)}}{r_s \text{ (m)}} \right)^2. \quad [10]$$

Neutral beams injected with higher energies will tend to make excursions outside the separatrix, and be less than ideal for FRC current drive or flux sustainment.

Other possible orbits can be examined by considering the conserved (in the absence of collisions and electric fields) canonical momentum

$$P_\theta = m_i r v_\theta + e\psi \quad [11]$$

and the total kinetic energy

$$H = \frac{1}{2} \left( v_r^2 + v_z^2 + \left( \frac{P_\theta - e\psi}{m_i r} \right)^2 \right) \quad [12]$$

For tangential injection and ionization with  $v_\theta = -v_b$  and negative  $\psi$ ,  $P_\theta = -(m_i R v_b + e(-\psi))$ . (Eq. (10) is derived from calling  $H = E_{ic} = m_i v_{ic}^2/2$ , calculating  $P_\theta$  for  $v_\theta = -v_{ic}$ ,  $r = R$ , and  $\psi = -\phi_p/2\pi$ , and substituting these values in Eq. (12) for excursions to  $\psi = 0$ ,  $r = r_s = \sqrt{2}R$  with  $v_r, v_z = 0$ .) The maximum radial extent of any orbit can be determined by setting  $v_r^2 + v_z^2 = 0$  in Eq. (12), requiring that  $\{(-P_\theta) + e\psi\}/m_i r < v_b$ . An example (B) with  $v_\theta = v_{im}$  and  $E_{im} = 0.5m_i v_{im}^2 = E_{ic}/5.8$  is also shown in Fig. 4, which is also typical of bulk ions making retrograde orbits in low flux FRCs.

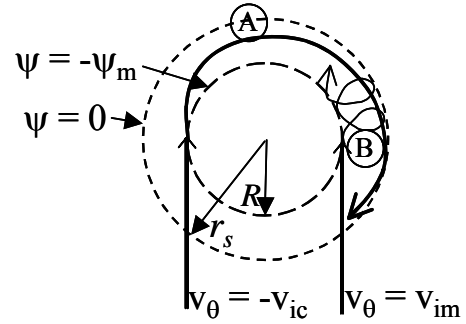


Figure 4. Critical energetic ion orbits in FRCs.

The Monte-Carlo calculations, including ionization, slowing down, and scattering can be compared with an ideal estimate assuming that all of the TNBI beam ‘current’  $I_b$  is ionized, captured, and makes axis encircling orbits with gyro time  $\tau_g = 2\pi R/v_b$ . That would result in a ring current

$$I_r \approx \frac{v_b \tau_s}{2\pi R} I_b \quad [13]$$

where the beam velocity  $v_b(\text{m/s}) = 3.1 \times 10^5 (E_b(\text{keV})/A_i)^{1/2}$  and the fast ion slowing down time

$$\tau_s(\text{s}) \approx \frac{0.02}{n_e(10^{20} \text{m}^{-3})} (T_e(\text{keV}) + 0.27 E_b(\text{MeV}))^{3/2} \quad [14]$$

Ignoring the  $E_b$  contribution to  $\tau_s$ , and taking an average beam velocity of  $(4E_b/3m_i)^{1/2}$  to account for the ion beam time history before thermalizing, the ideal ring to beam current ratio is

$$\alpha_{rb} = \frac{I_{ring}}{I_b} \approx 0.75 \frac{T_e^{3/2}(\text{keV}) E_b^{1/2}(\text{keV})}{A_i^{1/2} n_e(10^{20} \text{m}^{-3}) R(\text{m})} \text{ kA/A.} \quad [15]$$

$E_{ic} < 1$  keV in TCSU and is far too low for TNBI trapping at reasonable beam energies of 10 keV and above. If  $r_s$  is increased to 0.9 m and  $B_e$  to 60 mT ( $\phi_p \approx 45$  mWb),  $E_{ic}$  would be 18 keV. This magnetic field and flux level can be achieved by RMF in a larger,  $r_c \sim 1$  m device, even without decreases in the TCSU inferred resistivities by increasing  $B_o$  to 10 mT, which is a reasonable design point for a next experiment. The FRC peak density would be  $n_m = 1.5 \times 10^{19} \text{m}^{-3}$ , assuming a total temperature of  $T_i = 650$  eV can be reached. For the calculations a uniform  $T_e = T_i = 325$  eV is assumed. In a simple uniform 60 mT magnetic field the ion gyroradius for a 10 keV deuterium ion is 34 cm, which is an ideal situation since charge-exchange ions can easily remain inside the FRC 90 cm separatrix radius, but also encircle the FRC axis due to the lower magnetic field internal to the separatrix (effective fast ion trap). The fast ion slowing down time will be of order 10-20 msec, and any planned experiment should provide for timescales of at least that order.

Initial TNBI calculations were made for tangential injection at an impact parameter  $b = R$  (0.64 m for the above case) using a Grad-Shafranov equilibria with  $\ell_s \sim 5r_s$ . Results are shown by the solid line in **Fig. 5** as a function of deuterium beam energy  $E_b$ . Many particles were tracked, with ionization occurring at various points along the chord, yielding different initial values of  $v_\theta$ ,  $v_r$  and  $v_z$ . Since scattering is included in these calculations, the orbits change from ideal paths, and some ions

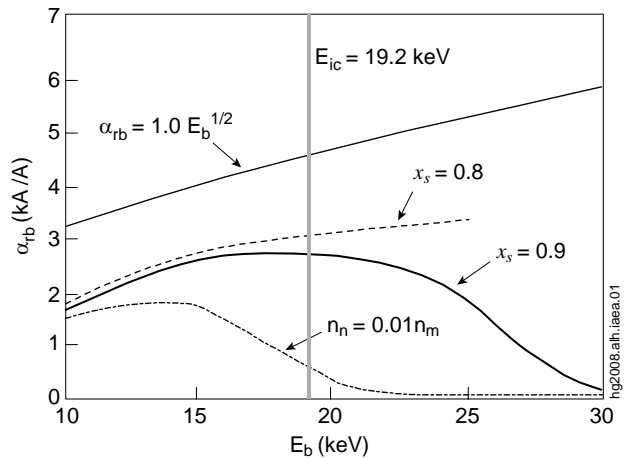


Figure 5. TNBI efficiency for 60 mT FRC with  $b = 0.64$  m.



will make excursions outside the separatrix even with  $E_b < E_{ic}$ . For the  $b = R$  injection about 2/3 of the neutral beam was ionized. The vacuum tube wall was specified as  $r_c = 1.0$  m ( $x_s = 0.9$ ) and beams with energies much beyond  $E_{ic}$  produced ions that increasingly intersected the wall, producing decreasing ratios of ring to beam current. This could be alleviated by having the wall further away (not ideal for RMF operation) as shown by the dashed  $x_s = 0.8$  curve in Fig. 5, but this is only effective if the neutral density outside the separatrix is low since the fast ions will rapidly charge-exchange with neutrals and be lost. The dash-dotted curve in Fig. 5 shows the effect of 1% neutrals ( $n_n = 1.4 \times 10^{17}$  m<sup>-3</sup>) outside the separatrix. The ion-neutral charge-exchange cross-section is about  $8 \times 10^{-20}$  m<sup>2</sup>, giving a mean free path of about 100 m. For a 20 keV ion travelling at  $\sim 10^6$  m/s, the slowing down time is about 25 msec, so it normally would travel about 25,000 m. The average distance ions which are lost to charge exchange with the outside neutrals travel is only 2,500 m ( $\sim 100$  m of which is outside the separatrix), which accounts for the large reduction in ring current generation. It is thus desirable to keep the neutral beam energy less than  $E_{ic}/2$ , especially when considering some neutral penetration inside the separatrix.

An ideal curve based on Eq. (15) is also shown by a dotted line. For  $E_b = 20$  keV the ideal  $\alpha_{rb}$  is 4.5 kA/A, or 3 kA/A when considering that only 2/3 of the neutral beam is ionized. The Monte-Carlo calculated  $\alpha_{rb} = 2.5$  kA/A value in Fig. 5 reflects more realistic orbits. Equation (15), adjusted for TNBI ‘shine-through’, can be used for approximate scaling analysis. It is also important that the beam energy exceed the electron temperature by about a factor of 50, or the slowing down time will be reduced due to collisions with ions.

The dependence on injection position is shown in Fig. 6. It is slightly more advantageous to inject at  $b > R$  since the average canonical angular momentum ( $-P_\theta$ ) will be larger, but for the Fig. 5,6 conditions this is compensated by a lower fraction of the beam being ionized. Such effects depend on the density-length product, but injecting with  $b$  between  $R$  and  $1.15R$  ( $\Delta b \sim 10$  cm for the  $r_s = 0.9$  m FRC) is probably optimal for most TNBI scenarios.

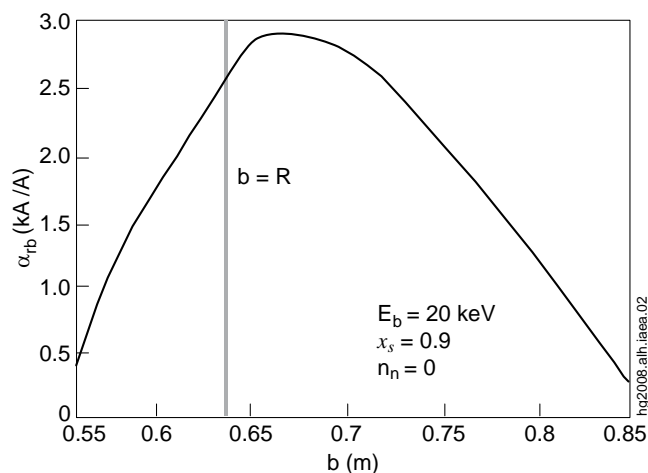


Figure 6. TNBI efficiency for 60 mT FRC as a function of impact parameter.

#### 4. Summary and Conclusions

RMF is an appropriate way to generate the field reversed configurations appropriate for TNBI charge-exchange ion trapping, and the combination of RMF and TNBI would be an ideal combination for providing FRC stability and current drive. Even without decreases in present plasma resistivity, ideal energetic ion traps for 10 keV ions can be produced in a device 2.5 times larger than TCSU. If even a less than expected four-fold drop in average

resistivity is experienced (which would be necessary for the experiment to be considered a success), the plasma flux and density would double (eliminating the TNBI shine-through losses), allowing for a doubling of the plasma temperature.  $E_{ic}$  would increase to 72 keV, resulting in an  $\alpha_{rb}$  of 10 kA/A at an  $E_b$  value of 40 keV. 50 A beams (2 MW) could then produce 500 kA of ion ring current, half of the total FRC azimuthal current.

For a small FRC/FRM reactor ( $r_s \sim 2$  m,  $n_e \sim 2 \times 10^{20}$  m<sup>-3</sup>) it would be necessary to have  $D_{\perp}$  values of order or less than 1  $\mu\Omega$ -m. This resistivity would be achieved if the TCSU drift-wave governed turbulence continues to apply, even without the expected benefits of TNBI. TNBI calculations for 10 keV temperatures show that  $\alpha_{rb}$  values of 100-200 kA/A are achievable, but only at  $E_b$  values above 1 MeV. Such high neutral beam energies are needed to provide sufficient beam penetration. A  $r_c = 1$  m,  $B_0 = 10$  mT experiment with neutral beams would go a long way, at a modest cost, to proving the viability of such an approach.

- [1] G.A. Carlson, et. al., "Conceptual design of the FRM reactor", Lawrence Livermore Laboratory Report UCRL-52467 (May 19, 1978).
- [2] B.G. Logan, et. al., "High- $\beta$ , gas-stabilized, mirror-confined plasma" Phys. Rev. Lett. **37**, 1468 (1976).
- [3] I.R. Jones, "A review of RMF current drive and the operation of the rotamak as FRC and a ST", Phys. Plasmas **6**, 1950 (1999).
- [4] A.L. Hoffman, H.Y. Guo, J.T. Slough, S.J. Tobin, L.S. Schrank, W.A. Reass, and G.A. Wurden, "The TCS RMF FRC current drive experiment", Fusion Science and Technology **41**, 92 (2002).
- [5] H. Y. Guo, A. L. Hoffman, and R. D. Milroy, "RMF current drive of high-temperature FRCs with high zeta scaling", Phys. Plasmas **14**, 112502 (2007).
- [6] R.D. Milroy, K.E. Miller, "Edge driven RMF current drive of FRCs ", Phys. Plasmas **11**, 633 (2004).
- [7] P.C. Liewer, R.C. Davidson, "Sheath broadening by the LHD instability in post implosion theta pinches", Nucl. Fusion **17**, 85 (1977).
- [8] R.D. Milroy, J.T. Slough, "Poloidal flux loss and axial dynamics during the formation of a FRC", Phys. Fluids **30**, 3566 (1987).
- [9] R.C. Davidson, N.A. Krall, "Anomalous transport in high-temperature plasmas with applications to solenoidal fusion systems" Nucl. Fusion **17**, 1313 (1977).
- [10] J. Loverich, U. Shumlak, "Nonlinear full two fluid study of the  $m=0$  sausage instabilities in an axisymmetric Z pinch", Phys. Plasmas **13**, 082310 (2006).
- [11] B. Rogers, "Gyrokinetic simulations of plasma turbulence, transport, and zonal flows in a closed field line geometry", Bull. Am. Phys. Soc. **52**, paper G12-4 99 (Nov. 2007).
- [12] T. Cho, "High confinement in fusion oriented plasmas with kV-order potential, ion, and electron temperatures with controlled radial turbulent transport in GAMMA 10", Bull. Am. Phys. Soc. **52**, paper G12-6 100 (Nov. 2007).
- [13] A.F. Lifschitz, R. Farengo, A.L. Hoffman, "Calculations of TNBI current drive efficiency for present moderate flux FRCs", Nucl. Fusion **44**, 1015 (2004).